Research Article **Open Access**

Jesús I. Tapia and Mildred Quintana*

Carbon Nanostructures Produced by Liquid Phase Exfoliation of Graphite in the Presence of Small Organic Molecules

DOI 10.1515/mesbi-2016-0010
Received June 23, 2016; revised October 19, 2016; accepted November 12, 2016

Abstract: We report on the formation of different carbon nanostructures by ultrasonication of graphite in DMF upon the addition of 3 different small molecules: ferrocene carboxylic acid, dimethylamino methyl-ferrocene, and benzyl aldehyde. Our results confirm that acoustic cavitation in organic solvents generates free radicals which enable or are involved in secondary reactions. During the ultrasonication process, the addition of small molecules induces the formation of different carbon nanostructures mainly depending on the chemical nature of the molecule, as observed by transmission electron microscopy (TEM). Raman spectroscopy analysis confirms that small molecules act as radical scavengers reducing the damage caused by cavitation to graphene sheets producing long nanoribbons, squared sheets, or carbon nanoscrolls. Importantly, this strategy allows the production of different carbon nanostructures in liquid-phase making them readily available for their chemical functionalization or for their incorporation into hybrids materials enabling the development of new advanced biological applications.

Keywords: graphene, nanoribbons, nanoscrolls, acoustic cavitation, ultrasonication

1 Introduction

Carbon is one of the more versatile elements in the Periodic Table. It is present in many allotropic forms namely diamond, graphite, amorphous carbon and nanostructures such as fullerenes, carbon nanotubes (CNTs) and graphene [1]. During recent years, the production of graphene by micromechanical cleavage [2] has triggered enormous experimental activity demonstrating that graphene monolayers possesses novel structural, [3] electrical [4] and mechanical [5] properties. Additionally, graphene is a 2D building material for other carbon nanostructures of all dimensionalities. Graphene can be wrapped up into 0D buckyballs, rolled into 1D nanotubes or stacked into 3D graphite crystals [6]. For example, *in situ* transmission electron microscopy (TEM) experiments demonstrated the direct transformation of small graphene fragments into fullerene cages [7], the ultrasonication of graphene in the presence of ferrocene aldehyde produce the formation of CNTs [8], while the ultrasonication of graphene in the presence of fullerene results in the formation of carbon nano onions and nanodiamond [9].

The synthesis of different types of carbon nanostructures in liquid phase is extremely important for the development of exciting biological applications including biosensors and synthetic nanopores. Graphene nanoribbon carpets exhibit a significantly higher sensitivity in electrically detecting adenosine triphosphate (ATP) molecules as compared to that of single-walled carbon nanotube networks [10]. Graphene nanopore sensors, which reside on an insulating membrane with molecular diameter, can be used as single molecule or even intramolecular detectors [11], and carbon nanoscrolls has been suggested as tunable water and ions channels, as well as synthetic pores for gene and drug delivery systems [12]. In this direction, ultrasonic techniques are an extremely powerful means in the synthesis, modification and manipulation of carbon nanomaterials [13]. Ultrasonication processes produce acoustic cavitation able to functionalize the CNT surface, open its ends or even fracture them completely [14]. Additionally, carbon nanotubes have been prepared from organic solvents with the assistance of ultrasound [15]. There are few definitive studies on the mechanism of cavitation-induced fragmentation of car-

Jesús I. Tapia: Instituto de Física, Universidad Autónoma de San Luis Potosí, Manuel Nava 6, Zona Universitaria, San Luis Potosí, SLP 78290, Mexico
***Corresponding Author: Mildred Quintana:** Instituto de Física, Universidad Autónoma de San Luis Potosí, Manuel Nava 6, Zona Universitaria, San Luis Potosí, SLP 78290, Mexico, E-mail: mildred@ifisica.uaslp.mx

bonaceous materials. It is well known that exfoliation of graphite in organic solvents takes place when the free energy of mixing is negative [16]. Another key requirement for a solvent to efficiently exfoliate graphite, is its ability to colloidally stabilize graphene [17]. Then, graphene-solvent interactions should be sufficiently strong to compensate the van der Waals attractive interactions between graphene sheets [18]. So far, it is accepted that acoustic cavitation essentially breaks the graphitic basal structure producing graphitic carbon fragments of variable size, which are later intercalated by solvent molecules causing exfoliation [19].

On the other hand, acoustic cavitation is responsible for both sonochemistry and sonoluminiscence [20]. When a solution is irradiated with ultrasound, the applied field can drive chemical reactions with high-energy intermediates produced by cavitation [21, 22]. Normally, cavitation in organic solvents generates free radicals, which can enable or be involved in secondary reactions [23]. For example, methyl radicals were detected during ultrasonication of DMF, rendering SWNT dispersions unstable [24]. Such a chemical attack may result in a size reduction of graphene layers and therefore be detrimental for their physical properties. To avoid this, the decomposition behaviour of the solvents and selected precursors need to be considered. Graphene dispersions produced by exfoliation of graphite in organic solvents such as *N*-methyl-2-pyrrolidone (NMP) and *N*, *N*–dimethylformamide (DMF) first reached concentrations up to 0.01 mg/ml and 1 wt% monolayer [16]. Later, increasing the sonication time, the concentration was increased up to 1.2 mg/ml with 4 wt% monolayer [25]. Unfortunately, after long ultrasonication treatments the resultant graphene layers present higher concentration of defects and reduction of the size directly proportional to the sonication time. Previous studies have demonstrated that sonication in DMF produces $^{\bullet}CH_3$ and $^{\bullet}CH_2N(CH_3)CHO$ radicals [26]. These radicals are formed either through reactions of the solutes with ultrasound-generated $^{\bullet}H$ and $^{\bullet}OH$ radicals, or by direct pyrolysis of the weak bonds in the solute molecules. In air-saturated sonicated solutions it was observed that these carbon targeted radicals are converted into the corresponding peroxyl radicals such as $^{\bullet}OOCH_2N(^{\bullet}CH_3)CHO$ [26].

To avoid oxidation, antioxidant molecules, for instance natural flavonoids [27], or small molecules as tiopronin [28] are employed to effectively inhibit the formation of the free radicals generated during ultrasonication in DMF. In the present work, we sonicated graphite in DMF with the addition of tree different small molecules: ferrocene carboxylic acid, dimethyl amino methyl-ferrocene, and benzyl aldehyde. Our results indicate the occurrence of different chemical processes during the sonication treatment. The presence of ferrocene carboxylic acid, dimethyl amino methyl-ferrocene, and benzyl aldehyde, induces differences in the cutting of the graphene layers producing carbon nanoribbons, “few layers graphene” (FLG) and the rolling of the graphene layers into carbon nanoscrolls, respectively.

2 Experimental Procedures

2.1 Characterization techniques

The optical characterization was carried out by UV-vis spectroscopy with a Cary 500 spectrophotometer using 10 mm path length quartz cuvettes. TEM measurements were performed with a TEM Philips EM208, using an accelerating voltage of 100 kV. Samples were prepared by drop casting from the dispersion onto a TEM grid (200 mesh, Nickel, carbon only). Raman spectra were recorded with an Invia Renishaw microspectrometer equipped with a laser at 532 nm using the 100 X objective. Samples were prepared by drop casting of the dispersion on silicon oxide surfaces (Si-Mat silicon wafers, CZ) allowing the solvent to evaporate. For Raman analysis, 30 spectra were taken of each sample.

2.2 Sample preparation

Samples were prepared using an ultrasonic tip processor GEX 750. All samples were sonicated in cycles of 30 s on / 30 s off for intervals of 3 h at the lower power of the ultrasonic tip (20%, 150 W). During ultrasonication, samples were kept in an ice bath to avoid overheating. 10 mg of graphite crystals (Bay Carbon, Inc. SP-1 graphite powder, www.baycarbon.com) were ultrasonicated in 30 ml of DMF during 1 h to induce partial exfoliation of graphite producing **G-1**. After sonication, dispersions were left to stabilize for 5 min and then the liquid phase was removed by pipetting. Dispersions were copiously washed by filtration with fresh DMF to remove all the possibly altered DMF. Special attention was paid to keep the samples wet during the filtration processes. Then, in different sets of experiments, 40 mg of ferrocene carboxylic acid, dimethyl amino methyl-ferrocene, or benzyl aldehyde were added to **G-1** in order to obtain **G-2**, **G-3**, and **G4,** respectively. Dispersions were further sonicated for 3 h, under the same experimental conditions. Finally, products were copiously washed by filtration with fresh DMF in order to remove the molecules

and by-products. Samples were re-dispersed in a bath ultrasonicator (few seconds) in 10 ml of fresh DMF. Centrifugation of all dispersions was carried out at 3000 rpm during 30 min. A precipitate was observed only for **G-1**.

3 Results and Discussion

UV-vis spectroscopy was used to measure the absorption at 660 nm. The concentration of the final dispersion was calculated using the absorption coefficient α = 2460 ml/mg·m, reported in ref. [16], resulting in 0.031±0.003 mg/ml for **G-1**. The dispersed material was investigated by TEM, as shown in Figure 1. TEM analysis (30 micrographs) indicates the presence of graphene flakes with lateral size of typically a few µm, consisting of several layers. Raman spectroscopy captures the fingerprint of the different carbon nanostructures [30], the most important parameters for each sample are reported in Table 2. The quality of **G-1** was analysed by Raman spectroscopy, reported in Figure 2. The 2D band at 2689 cm^{-1} for **G-1** consists of two components typical of the structure of crystalline graphite and the ABAB stacking [29]. This result therefore agrees very well with the existence of multilayer graphene flakes firstly detected by TEM. These D/G intensity ratio (I_D/I_G) was found to be 0.37, identifying **G-1** as graphene aggregates relatively free of defects, see Table 3. After complete characterization of the starting material, **G-2, G-3** and **G-4** were obtained separately by sonication of **G-1** with the addition of ferrocene carboxylic acid (**G-2**), dimethyl amino methyl-ferrocene (**G-3**), and benzyl aldehyde (**G-4**), respectively as shown in Table 1 and Figure 3. After washing and re-dispersing the products **G-2**, **G-3** and **G-4** in 10 ml of fresh DMF, the concentration of the samples were calculated from the optical absorption as described above for **G-1** and found to be 0.029±0.010 mg/ml for all of them. TEM examination of **G-2** indicates the presence of very long graphene nanoribons (35 ±0.5 µm) observed in Figure 4a and in 4b at higher magnification. Instead, for **G-3** the cutting of the layers produced squared sheets (200±100 nm per side), as observe in Figure 4c and 4d. For **G-4**, the addition of benzyl aldehyde induces the formation of carbon nanoscrolls shown in 4e and 4f.

The Raman spectrum of **G-2**, **G-3** and **G-4** are shown in Figure 5 and the main parameters are reported in Tables 2 and 3. The G and 2D bands are shown in Figures 6 and 7, the full width at half maximum (FWHM) broadening in all the Raman signals is due to disorder. An evaluation of the concentration of defects present on graphene sheets was carried out by computing the intensity of the D

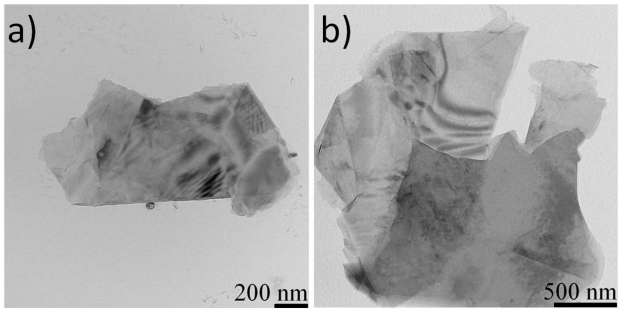

Figure 1: TEM micrographs of solution cast **G-1**.

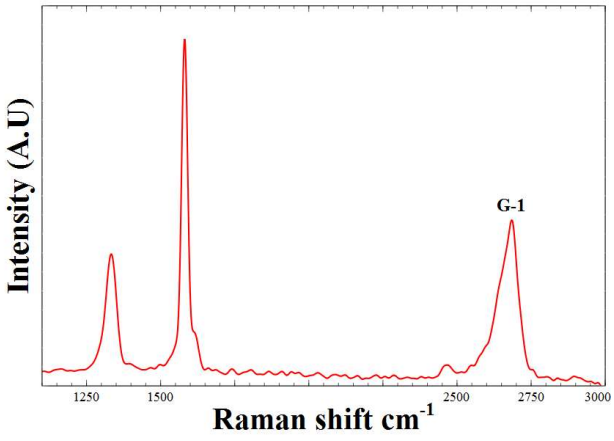

Figure 2: Raman spectra of **G-1**.

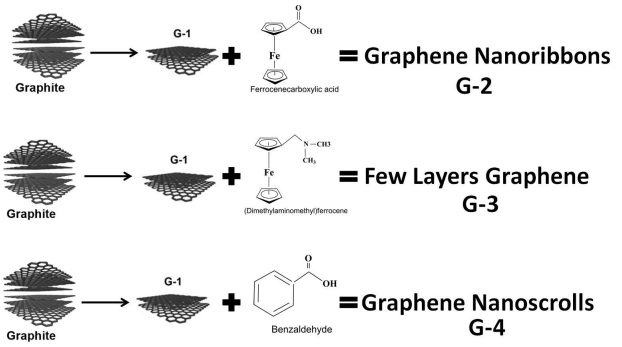

Figure 3: Ultrasound-assisted synthesis of **G2**, **G3** and **G4**.

peak at 1332 cm^{-1} relative to the G peak (~1580 cm^{-1}). The I_D/I_G values were calculated obtaining 0.854, 0.852 and 0.857, respectively, see Table 3. For **G1** and **G2**, the symmetrical shape of the 2D peak (no shoulder as in graphite) evidences the existence of graphene (Figure 7). The occurrence of a small D band at 1346 nm^{-1} and the small I_D/I_G value are attributed to the edges of the graphene nanoribbons **G-2**, and nanosheets **G3**. The 2D-band is symmetrical and roughly consists of one component, typical of monolayer or few-layer graphene, Figure 7 [30]. The presence of the band at 1625 nm^{-1}, commonly named R' band, is a sig-

Table 1: Samples codes and experimental details.

Experiment	Description
G-1	Graphite crystals ultrasonicated in DMF for 1 hour in order to obtaining "few layers graphene" (FLG)
G-2	Ferrocene carboxylic acid added to the dispersion containing FLG. Dispersions were sonicated for 3 h
G-3	Dimethyl amino methyl-ferrocene added to the dispersion containing FLG. Dispersions were sonicated for 3 h.
G-4	Benzyl aldehyde added to the dispersion containing FLG. Dispersions were sonicated for 3 h.

Table 2: Raman bands parameters and FWHMs.

Sample	D peak λ_{Max} (cm^{-1})	G peak λ_{Max} (cm^{-1})	2D peak λ_{Max} (cm^{-1})	FWHM D peak (cm^{-1})	FWHM G peak (cm^{-1})	FWHM 2D peak (cm^{-1})
Graphite	1355.45	1579.02	2716.14	16.312	7.384	16.020
G-1	1333.39	1579.99	2684.43	24.226	12.629	33.414
G-2	1349.746	1575.601	2697.641	22.614	12.426	55.768
G-3	1348.721	1581.444	2699.895	24.612	9.814	52.474
G-4	1361.31	1598.88	2703.539	26.603	8.790	52.809

Table 3: I_D/I_G ratio and in plane correlation length (L_D).

Sample	I_D/I_G	L_D (nm)
Graphite	0.021	1.95 *
G-1	0.37	8.20*
G-2	0.854	22.51**
G-3	0.852	22.56**
G-4	0.857	22.43**

* The values were calculated in the low defect-density regime.

** The values were calculated using the high defect-density regime.

nal for superlattices in bilayer graphene and its properties depend on mismatch rotation angle [31]. The occurrence of the R' band in **G-3** suggests the presence of twisted few layers graphene and confirms the production of nanoscrolls in **G-4**.

The Raman analysis of the samples is summarized in Table 2 and 3. In order to compare the different samples the amount of disorder and turbostraticity are important parameters. Using I_D/I_G ratio, the level of disorder presents two different behaviours. There is a regime of "low" defect density where I_D/I_G increases creating more elastic scattering, while in the "high" defect density I_D/I_G originates from the increases in the amorphous carbon structure or turbostraticity. Thus, the I_D/I_G ratio and the in plane correlation length (L_D), corresponded to the average inter-defect distance, are approximated by two empirical formulas for the two separated regimes [30], values are reported in Table 3. For all the samples in the "high" defect density regime **G-2**, **G-3** and **G-4**, L_D ($\sim$22 nm) indicates the presence of defects, including bond length and angle disorder at the atomic scale and in plane and edges sp^3 bonds. It has been notice that turbostratic graphite (without the planar AB stacking) has a single 2D peak [30] as the one observed for **G-2, G-3** and **G-4**. However, the 2D FWHM for these samples is $\sim$50 cm^{-1} considerably higher than the 2D peak of graphene and shifted $\sim$20 cm^{-1}. These values corroborate the presence of turbostratic graphite demonstrating the exfoliation of graphite in the production of graphene nanoribbons, few layers graphene, and carbon nanoscrolls.

The sonication of graphite without the addition of additives such as small molecules under the same experimental conditions produces a low intensity 2D band associated with damaged graphene and the I_D/I_G value of 0.99, identify the material as highly damaged graphene comparable to graphene oxide [8]. Molecular additives certainly play a crucial role in producing different type of carbon nanostructures during ultrasonication processes.

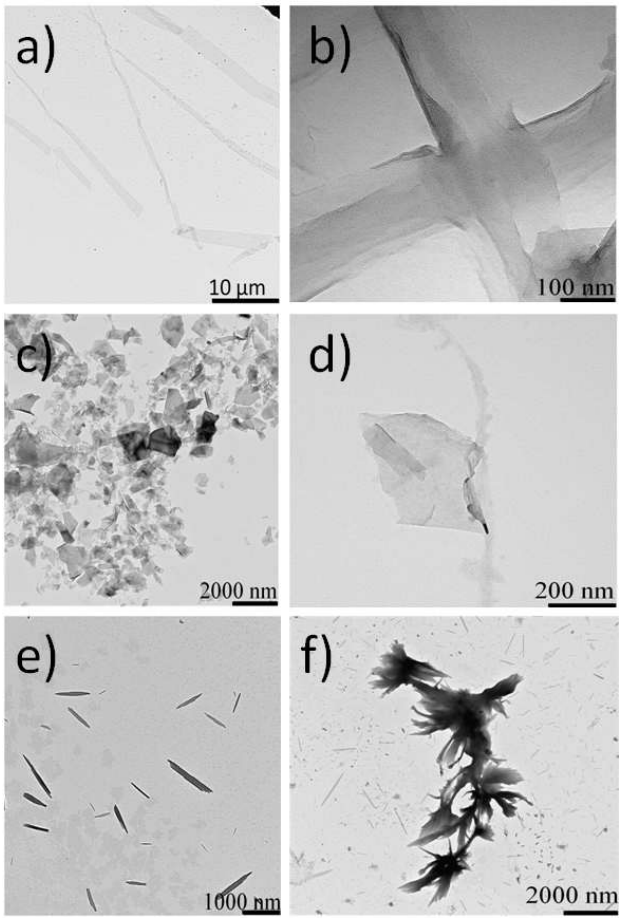

Figure 4: Representative TEM micrographs of **G2** (a and b), **G3** (c and d) and **G4** (e and f).

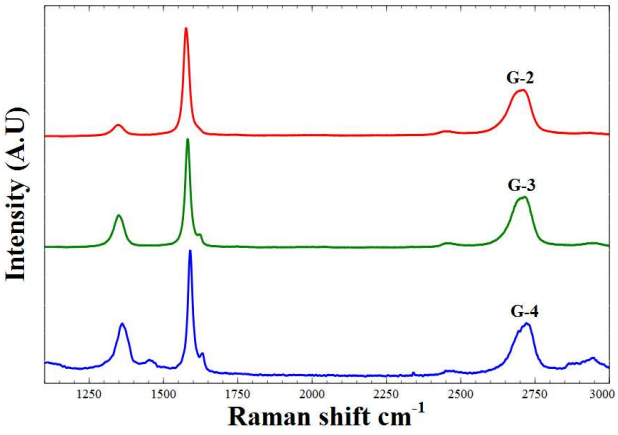

Figure 5: Raman spectra of drop-cast **G-2**, **G3**, and **G-4**.

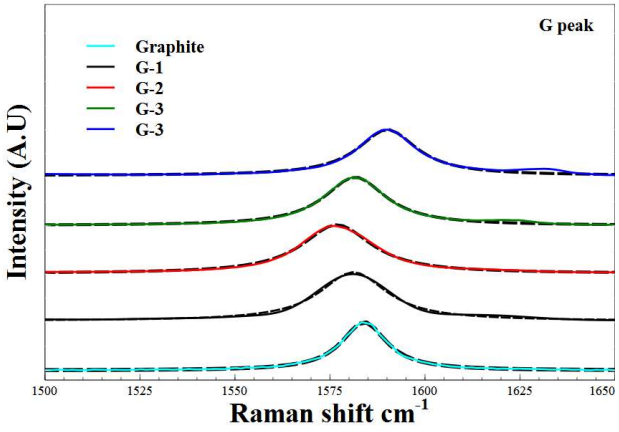

Figure 6: Comparison of the FWHM of the G Band.

4 Conclusions

From all these observations, we suggest that during ultrasonication without the addition of additives, acoustic cavitation formed radical species strong enough to gradually oxidize the entire graphene sheet. This process might be initiated at the edges and inner defects cutting graphene sheets in small pieces. Conversely, during sonication of graphite with the addition of small molecules, the radical reactive species produces by acoustic cavitation are considerably reduced, probably as consequence of radical attack starting from small molecules. However, some radical attack to the edges occurs creating a kind of cooperative effect. The latter can be explained as follows: depending on the cutting direction of graphene, two unique types of edges can be obtained: zigzag and armchair. The geometry of the edge makes an enormous difference in the π-electron structure at the edge [32]. Spin-polarized π-electrons are localized on the zigzag carbon atoms conferring them *partial radical* character and thus special chem-

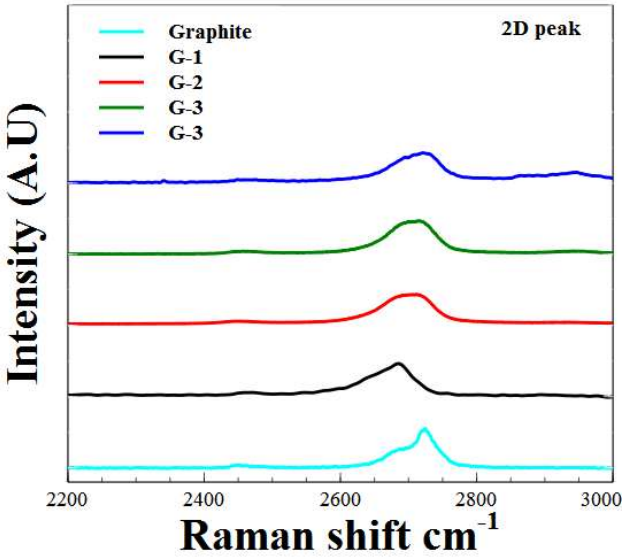

Figure 7: Comparison of the FWHM and shape of the 2D Band.

ical reactivity. These electrons are not confined but can act collectively when interacting with another radical [33]. We suspect that the zig-zag cutting of graphene is preferred by the mild radical attack producing thin graphene nanoribbons. Theory indicates that carbon nanoscrolls are formed when a critical overlap between sheet layers is achieved for partially curled sheets [34]. Thus rolling up the nanoribbons will increase their stability as a result of the van der Waals contributions. Summarizing, the effect of adding small molecules during exfoliation of graphite by ultrasonication in DMF was investigated. The formation of nanoribbons, squared sheets and nanoscrolls was observed. These results are expected to pave the way for the development of advanced biological applications such as artificial pores and biodetection systems based on carbon nanostructures.

Acknowledgement: This research was supported by Conacyt CB-166014, I-225984. Thanks are given to M. C. Lourdes González-González and Dra. Aurora Robledo for technical support.

References

[1] C.N.R. Rao, R. Seshadri, A. Goviandaraj, R. Sen, Fullerenes, nanotubes, onions and related carbon structures, Materials Science and Engineering: R: Reports 15, 1995, 209.

[2] K.S. Novoselov, A.K. Geim, S.V. Morozov, D. Jiang, Y. Zhang, S.V. Dubonos, I.V. Grigorieva, A.A. Firsov, Electric field effect in atomically thin carbon films, Science 306, 2004, 666.

[3] J.C. Meyer, A.K. Geim, M.I. Katsnelson, K.S. Novoselov, T.J. Booth, S. Roth, The structure of suspeded graphene sheets, Nature 446, 2007, 60.

[4] N.Castro, F.Guinea, N.M.R. Peres, K.S. Novoselov, A.K. Geim, The electronic properties of graphene, Reviews of Modern Physics, 81, 2009, 109.

[5] I.W. Frank, D.M. Tanenbaum, A.M. van der Zande, P.L. McEuen, Mechanical properties of suspended graphene sheets, Journal of Vacuum Science & Technology, 25, 2007, 2558.

[6] A.K. Geim, K.J. Novoselov, The rise of graphene, Nature Materials, 6, 2007, 183.

[7] A. Chuvilin, U. Kaiser, E. Bichoutskaia, N. Besley, A.N. Khlobystov, Direct transformation of graphene to fullerene, Nature Chemistry, 2, 2010, 450.

[8] M. Quintana, M. Grzelczak, K. Spyrou, M. Calvaresi, S. Baals, B. Kooi, G.Van Tendeloo, P. Rudolf, F. Zerbeto, M. Prato, A Simple road for the transformation of few-layers graphene into MWNTs, Journal of the American Chemical Society, 134, 2012,13310.

[9] J.I. Tapia, M. Quintana, E. Larios, C. Bittencourt, M.J. Yacaman, Carbon nano-allotropes produced by ultrasonication of few-layer graphene and fullerene, Carbon, 99, 2016, 541.

[10] X. Dong, Q. Long, J. Wang, M. B. Chan-Park, W. Huang, P. Chen, A graphene nanoribbon network and its biosensing applications, Nanoscale, 3, 2011, 5156.

[11] C. A. Merchant, K. Healy, M. Wanunu, V. Ray, N. Peterman, J. Bartel, M. D. Fischbein, K. Venta, Z. T. Luo, A. T. C. Johnson, M. Drndic, DNA Translocation through Graphene Nanopores, Nano Letters, 10, 2010, 2915.

[12] X. Shi, Y. Cheng, N. M. Pugno, H. Gao, Tunable Water Channesls with Carbon Nanoscrolls, Small, 6, 2010, 739.

[13] S.E. Skrabalak, Ultrasound assisted synthesis of carbon materials, Physical Chemistry Chemical Physics, 11, 2009, 4930.

[14] M. Kaempgen, M. Lebert, M. Haluska, N. Nicolso, S.Roth, Sonochemical optimization of the conductivity of single wall carbon nanotubes networks, Advanced Materials, 20, 2008, 616.

[15] M. Calvaresi, M. Quintana, P. Rudolf, F. Zerbetto, M. Prato, Rolling-up a graphene sheets, ChemPhysChem, 14, 2013, 3447.

[16] Y.Hernandez, V. Nicolosi, M. Lotya, F.M. Blighe, Z. Sun, S. De, I.T. McGovern, B. Holland, M. Byrne, Y.K. Gun'Ko, J.J. Boland, P. Niraj, G. Duesberg, S. Krishnamurthy, R. Goodhue, J. Hutchison, V. Scardaci, A.C. Ferrari, J.N.Coleman, High-yield production of graphene by liquid-phase exfoliation of graphite, Nature Nanotechnology, 3, 2008, 563.

[17] M. Quintana, J.I. Tapia, M. Prato, Liquid-phase exfoliated graphene: functionalization, characterization, and applications, Beilstein Journal of Nanotechnology, 5, 2014, 2328.

[18] C.J. Shin, S.Lin, M.S. Strano, Understanding the stabilization of liquid-phase-exfoliated graphene in polar solvents: Molecular dynamic simulations and kinetic theory of colloid aggregation, Journal of the American Chemical Society, 132, 2010, 14638.

[19] G. Cravotto, P. Cintas, Sonication-assisted fabrication and post-synthetic modifications of graphene like materials, Chemistry - A European Journal, 16, 2010, 5246.

[20] Y.T. Didenko, K.S. Suslick, The Energy Efficiency of Formation of Photons, Radicals and Ions During Single-Bubble Cavitation, Nature 418, 2002, 394.

[21] A. Gedanken, Using sonochemistry for the fabrication of nanomaterials, Ultrasonics Sonochemistry, 11, 2004, 47.

[22] K.S. Suslick, S.B. Choe, A.A. Cichowlas, M.W. Grinstaff, Sonochemical synthesis of amorphous carbon, Nature, 353, 1991, 414.

[23] M.W. Forney, J.C. Poler, Sonochemical formation of methyl hydroperoxide in polar aprotic solvents and its effect on single walled carbon nanotube dispersion stability, Journal of the American Chemical Society, 132, 2010, 791.

[24] V. Misik, P. Riesz, Peroxyl radical formation in aqueous solutions of N,N-dimethylformamide, N-ethylfomamide and dimethylsufoxide by ultrasound: Implications for sonosensitized cell killing. Free Radical Biology and Medicine, 20, 1996, 129.

[25] U. Khan, A. O' Neil, M. Loyta, S. De, J.N.Coleman, High-concentration solvent exfoliation of graphene, Small, 6, 2010, 864.

[26] V. Misik, P. Riesz, Peroxyl radical formation in aqueous solutions of N,N-dimethylformamide, N-ethylfomamide and dimethylsufoxide by ultrasound: Implications for sonosensitized cell killing. Free Radical Biology and Medicine, 20, 1996, 129.

[27] J. Wang, L.Y. Huang, G.A. Chen, J.L.Huang, The sonochemiluminiscence of lucigein in N,N- dimethylformamide solution under the influence of natural flavonoids, Chemistry Letters, 34, 2005, 1514.

[28] M. Quintana, M. Grzelczak, K. Spyrou, B. Kooi, S. Bals, G. Van Tendeloo, P. Rudolf, M. Prato, Production of large graphene sheets by exfoliation of graphite under high power ultrasound in the presence of tiopronin, Chemical Communications, 48, 2012,

12159.

[29] M. Endo, Y.A. Kim, Y. Fukai, T. Hayashi, M. Terrones, H. Terrones, M.S. Dresselhaus, Comparison study of semi-crystalline and highly crystalline multiwalled carbon nanotubes, Applied Physics Letters, 79, 2001, 1531.

[30] A.C. Ferrari, J. Robertson, Interpretation of the Raman spectra of disordered and amorphous carbon, Physical Review B, 61, 2000, 14095.

[31] V. Carozo, C.M. Almeida, E.H.M. Ferreira, L.G. Cançado, C.A. Achete, A. Jorio, Raman Signature of Graphene Superlattices, Nano Letters, 11, 2011 4527.

[32] K.Nakada, M. Fujita, G. Dresselhaus, M.S.Dresselhaus, Edge state in graphene ribbons: Nanometer size effect and edge shape dependence, Physical Review B, 54, 1996, 17954.

[33] D. Jiang, B.G. Stumper, S. Dai, Unique chemical reactivity of graphene nanoribbon's zigzag edge, The Journal of Chemical Physics, 126, 2007, 134701.

[34] S.F. Braga, V.R. Coluci, S.B. Legoas, R. Giro, D.S. Galvão, R.H. Baughman, Structure and dynamics of carbon nanoscrolls, Nano Letters, 4, 2004, 881.